Innovative: International Multi-disciplinary Journal of Applied Technology
(ISSN 2995-486X) VOLUME 04 ISSUE 04, 2026

CLASSIFICATION OF COMPLEX ANATOMICAL VARIANTS IN PEDIATRIC PATIENTS AFTER URANOPLASTY: AN INTEGRATED DIGITAL AND BIOCHEMICAL MONITORING APPROACH

Anvarova Muhtasar Anvarovna[1]
[1]*Samarkand State Medical University, Samarkand, Uzbekistan*
muxtasara46@gmail.com

Abstract:

Background: Cleft palate (CP) remains one of the most prevalent congenital craniofacial anomalies globally, affecting approximately 1 in 700 live births. Although uranoplasty restores anatomical continuity of the palate, post-surgical rehabilitation is frequently complicated by residual neuromuscular imbalances, altered occlusal dynamics, and compromised mucosal immune function. The absence of an integrated, multimodal monitoring framework limits the clinician's ability to detect and address these sequelae in a timely manner.

Objective: This study aimed to develop and validate an integrated classification of complex anatomical variants observed in post-uranoplasty pediatric patients, and to evaluate the effectiveness of digital monitoring combined with biopolymer aligner-based orthodontic therapy on neuromuscular, occlusal, and biochemical outcomes.

Methods: A prospective clinical observational study enrolled 150 children aged 6–12 years, divided into three groups of 50: a main group receiving digital monitoring with electromyography (EMG), T-Scan occlusal analysis, and biopolymer aligner therapy; a comparison group receiving conventional orthodontic treatment; and a healthy control group. Salivary biomarkers—alpha-amylase and secretory immunoglobulin A (sIgA)—were quantified at baseline and after 12 months. Statistical analysis employed the Mann–Whitney U test, Wilcoxon signed-rank test, and Spearman correlation (significance: $p<0.05$).

Results: At baseline, masseter peak amplitude in the main group was 118.4 ± 12.3 μV, representing a 2.1-fold reduction versus controls (247.3 ± 18.6 μV; $p<0.001$). Muscular asymmetry index reached 31.4 ± 3.4%. Total occlusion time was prolonged approximately fourfold (1.82 ± 0.21 s vs. 0.46 ± 0.06 s in controls; $p<0.001$). Salivary alpha-amylase was elevated 2.2-fold relative to healthy peers. After 12 months, the main group demonstrated statistically superior improvements in all parameters compared to the comparison group ($p<0.05$ for all outcomes).

Conclusion: Integrated digital monitoring combining EMG, T-Scan, and salivary biomarkers enables a precise, evidence-based classification of post-uranoplasty anatomical variants and substantially enhances rehabilitation outcomes. Early multimodal intervention is recommended for all pediatric patients following cleft palate repair.

Keywords: cleft palate; uranoplasty; electromyography; T-Scan occlusal analysis; salivary biomarkers; biopolymer aligners; neuromuscular rehabilitation.

1. Introduction

Cleft lip and palate (CLP) represents the most common congenital craniofacial anomaly, with a global incidence of approximately 1 per 700 live births, though considerable epidemiological variation exists across ethnic populations and geographic regions. In Central Asia, including Uzbekistan, the incidence is reported at 1.2–1.6 per 1,000 births, reflecting a combination of genetic predisposition, consanguinity patterns, and potential environmental contributors such as periconceptional nutritional deficiencies and teratogen exposure [1].

Surgical correction of the palatal defect through uranoplasty—most commonly performed between the ages of 9 and 18 months—aims to restore palatopharyngeal competence, facilitate normal speech development, and support adequate nasal breathing. However, surgical repair does not fully resolve the complex pathophysiological sequelae of the original malformation. Post-operative scar tissue formation, altered muscular insertions, and residual bone deficiencies collectively contribute to a spectrum of functional impairments affecting masticatory biomechanics, occlusal balance, and mucosal immunity [2].

Neuromuscular imbalances are particularly prominent in post-uranoplasty children. Electromyographic (EMG) studies have consistently demonstrated reduced activity amplitudes in the masseter and temporalis muscles, asymmetric co-contraction patterns, and prolonged masticatory cycle durations compared to age-matched healthy controls. These alterations are attributable to disruption of the palatoglossus and tensor veli palatini musculature during primary palatoplasty, as well as compensatory adaptive responses in orofacial motor programming. Untreated, these imbalances may perpetuate skeletal discrepancies, contribute to temporomandibular dysfunction, and adversely affect craniofacial growth trajectories [3].

Occlusal analysis using computerised force-measurement technologies such as the T-Scan system has refined understanding of contact timing and force distribution in these patients. Studies conducted in the United States, Japan, and several European centres have documented markedly prolonged total occlusal contact time, lateral force asymmetries, and anterior guidance disturbances in post-palatoplasty cohorts. These findings underscore the inadequacy of conventional clinical examination for characterising occlusal pathology in this population [4].

At the biochemical level, salivary composition in post-uranoplasty patients reflects both local mucosal stress and systemic metabolic alterations. Salivary alpha-amylase (sAA), a sensitive indicator of sympatho-adrenal activation and oxidative tissue burden, has been reported to be significantly elevated in children with craniofacial anomalies. Conversely, secretory immunoglobulin A (sIgA), the primary mucosal immunoglobulin, is frequently diminished, indicating compromised local immune surveillance. Despite the clinical relevance of these biomarkers, their integration into routine post-uranoplasty monitoring protocols remains limited [5].

A critical gap in current research is the absence of a validated, integrated framework that simultaneously captures neuromuscular, occlusal, and immunological dimensions of post-uranoplasty rehabilitation. Existing classification systems for anatomical variants in cleft palate are predominantly morphological, failing to incorporate functional and biological parameters that are essential for personalised treatment planning. Furthermore, the application of digital orthodontic technologies—including computer-aided aligner fabrication from biocompatible polymers—in this patient population has received insufficient systematic investigation [6].

The present study addresses this gap by developing and applying a novel integrated classification of complex anatomical variants in post-uranoplasty children and evaluating the additive benefit of

digital monitoring combined with biopolymer aligner therapy. The specific aims were: (1) to characterise baseline neuromuscular, occlusal, and biochemical profiles in post-uranoplasty children aged 6–12 years; (2) to assess changes in these parameters following 12 months of either digitally guided or conventional orthodontic management; and (3) to identify predictive biomarker correlations that may guide early and targeted intervention [7].

2. MATERIALS AND METHODS

2.1 Study Design and Ethical Approval

This prospective, parallel-group clinical observational study was conducted between January 2021 and December 2023 at the Department of Orthodontics and Maxillofacial Rehabilitation, Samarkand State Medical University. The study protocol was reviewed and approved by the Institutional Ethics Committee (Protocol No. 14/2021). Written informed consent was obtained from the parents or legal guardians of all participating children prior to enrollment, in accordance with the Declaration of Helsinki (2013 revision) [8].

2.2 Participants and Group Assignment

One hundred and fifty children aged 6–12 years who had previously undergone uranoplasty for non-syndromic cleft palate were recruited consecutively. All participants had completed primary surgical repair at least 24 months prior to enrollment and were dentally mature enough for functional assessment [9]. Exclusion criteria comprised: (i) syndromic conditions (e.g., Pierre Robin sequence, velocardiofacial syndrome); (ii) prior orthodontic treatment; (iii) systemic diseases affecting salivary function or immune status; (iv) concurrent use of medications influencing salivary composition; and (v) incomplete baseline data.

Participants were allocated to three groups of 50 by stratified randomisation using age (6–9 years vs. 10–12 years) and cleft laterality (unilateral vs. bilateral) as stratification variables. The main group (MG) received digitally monitored orthodontic treatment incorporating biopolymer aligner therapy. The comparison group (CG) received conventional removable or fixed orthodontic appliance therapy [10]. The control group (CTR) comprised 50 age- and sex-matched healthy children without any history of orofacial clefting, recruited from the university dental outpatient department for reference data only. Group characteristics are summarised in Table 1.

Table 1.Distribution and baseline characteristics of study participants (n=150)

Characteristic	Main Group (n=50)	Comparison Group (n=50)	Control Group (n=50)	Total (n=150)	p-value
Age 6–9 years, n (%)	24 (48%)	23 (46%)	25 (50%)	72 (48%)	0.912
Age 10–12 years, n (%)	26 (52%)	27 (54%)	25 (50%)	78 (52%)	0.912
Male, n (%)	28 (56%)	26 (52%)	27 (54%)	81 (54%)	0.867
Female, n (%)	22 (44%)	24 (48%)	23 (46%)	69 (46%)	0.867
Unilateral cleft, n (%)	36 (72%)	34 (68%)	—	70 (70%)	0.643
Bilateral cleft, n (%)	14 (28%)	16 (32%)	—	30 (30%)	0.643
Prior uranoplasty, n (%)	50 (100%)	50 (100%)	0 (0%)	100 (67%)	<0.001

Values are n (%). *p<0.001 vs. control group. MG = main group; CG = comparison group; CTR =

control group. Statistical comparison by chi-square test.

2.3 Electromyographic Assessment

Surface electromyography (sEMG) was performed using a standardised eight-channel EMG system (BioEMG III, BioResearch Associates, Milwaukee, WI, USA) with disposable pre-gelled Ag/AgCl electrodes positioned bilaterally over the masseter and anterior temporalis muscles. Electrode placement followed the SENIAM (Surface EMG for Non-Invasive Assessment of Muscles) guidelines. Signal acquisition was conducted at a sampling rate of 1,000 Hz with a bandpass filter of 20–500 Hz. Three consecutive 5-second standardised chewing sequences using a calibrated test food (Parafilm M, 0.5 g) were recorded per session and ensemble-averaged [11]. Peak amplitude (μV), left-right asymmetry index (%), and chewing cycle duration (ms) were extracted as primary outcome variables. Measurements were performed at baseline (T0) and after 12 months of treatment (T1).

2.4 T-Scan Computerised Occlusal Analysis

Dynamic occlusal analysis was performed with the T-Scan III system (Tekscan, Inc., South Boston, MA, USA), which records occlusal contact timing and relative force distribution as a function of time at a sensor sampling rate of 50 Hz. A standardised protocol required each participant to perform five maximum intercuspation closures. Total occlusal time (s), percentage of occlusal force distributed to the left and right sides, anterior guidance time (s), and centre of force (COF) displacement (mm) were recorded. Data were collected at T0 and T1, and compared against reference values from the CTR group [12].

2.5 Salivary Biochemical Analysis

Unstimulated whole saliva was collected using the passive drool method between 09:00 and 11:00 hours, at least 2 hours following the last food intake. Samples were centrifuged at 3,000 rpm for 10 minutes at 4°C, and supernatants were immediately aliquoted and stored at −80°C until analysis. Salivary alpha-amylase (sAA) activity was quantified using a colorimetric enzymatic assay kit (Salimetrics LLC, Carlsbad, CA, USA), with results expressed as U/mL. Secretory immunoglobulin A (sIgA) was measured by enzyme-linked immunosorbent assay (ELISA; Salimetrics LLC) and expressed as mg/L. Total protein content was determined by the Bradford method [13]. Malondialdehyde (MDA), a marker of lipid peroxidation and oxidative stress, was quantified by the thiobarbituric acid reactive substances (TBARS) assay. Lysozyme activity was assessed using a turbidimetric method with Micrococcus lysodeikticus substrate.

2.6 Digital Monitoring and Biopolymer Aligner Therapy

Participants in the MG underwent intraoral scanning (iTero Element 2, Align Technology, San Jose, CA, USA) at baseline and at 3-month intervals throughout the 12-month study period. Three-dimensional digital models were analysed using dedicated software (OrthoCAD v4.0) to quantify changes in palatal vault morphology, intercanine and intermolar widths, and dental arch perimeter. Biopolymer aligners were fabricated from medical-grade thermoplastic polyurethane (TPU) with a shore hardness of 65A, customised via computer-aided design and manufacturing (CAD/CAM) to apply targeted biomechanical forces. Aligners were worn for a minimum of 20 hours per day, with sequential changes planned according to digital simulation [14].

2.7 Statistical Analysis

All statistical analyses were performed using SPSS Statistics v26.0 (IBM Corp., Armonk, NY, USA). Data normality was assessed using the Shapiro–Wilk test. Because the majority of continuous variables exhibited non-normal distributions, non-parametric methods were applied throughout. Between-group comparisons at each time point were performed using the Mann–Whitney U test. Within-group longitudinal changes were evaluated using the Wilcoxon signed-rank test. Associations between EMG parameters and salivary biomarkers were quantified by Spearman rank correlation. Effect sizes were calculated as the rank-biserial correlation (r) for Mann–Whitney comparisons. The significance threshold was set at $p<0.05$ (two-tailed) for all tests. No multiple-comparison correction was applied given the exploratory nature of the study, but Bonferroni-adjusted results are noted where appropriate [15].

3. RESULTS

3.1 Electromyographic Findings

At baseline (T0), masseter peak amplitude in both patient groups was markedly reduced compared

to healthy controls (MG: 118.4 ± 12.3 μV; CG: 121.6 ± 13.7 μV; CTR: 247.3 ± 18.6 μV; p<0.001 for both inter-group comparisons). This represents an approximately 2.1-fold reduction relative to normative values, consistent with the hypothesis of chronic disuse atrophy and altered neuromuscular patterning following palatoplasty. Anterior temporalis muscle amplitudes were similarly reduced (MG: 102.1 ± 9.8 μV vs. CTR: 218.5 ± 16.9 μV; p<0.001).

The left-right asymmetry index was substantially elevated in both patient groups at T0 (MG: 29.7 ± 3.1%; CG: 31.4 ± 3.4%), compared to the physiological reference range observed in controls (6.3 ± 1.2%). In children with bilateral clefts, the asymmetry index reached values of up to 38.2%, reflecting disproportionate compensatory loading of the less affected masticatory side [16].

Following 12 months of treatment, the MG demonstrated statistically superior improvements compared to CG in masseter amplitude (198.7 ± 14.1 μV vs. 156.2 ± 15.4 μV; p<0.001; effect size r = 0.71), asymmetry index (14.2 ± 2.4% vs. 22.6 ± 2.9%; p<0.001), and chewing cycle duration (634 ± 39 ms vs. 679 ± 44 ms; p=0.012). EMG findings are presented in Table 2 and Figure 1.

Table 2. Electromyographic parameters (μV) at baseline (T0) and after 12 months (T1)

EMG Parameter	Main (Before)	Main (After)	Comparison (Before)	Comparison (After)	Control
Masseter peak amplitude, μV	118.4 ± 12.3	198.7 ± 14.1*	121.6 ± 13.7	156.2 ± 15.4*	247.3 ± 18.6
Temporal muscle amplitude, μV	102.1 ± 9.8	177.4 ± 12.6*	105.3 ± 10.4	143.8 ± 13.2*	218.5 ± 16.9
Left/Right asymmetry index, %	29.7 ± 3.1	14.2 ± 2.4*	31.4 ± 3.4	22.6 ± 2.9*	6.3 ± 1.2
Muscle activity ratio (M/T)	1.16 ± 0.09	1.12 ± 0.07	1.15 ± 0.10	1.14 ± 0.08	1.13 ± 0.05
Chewing cycle duration, ms	712 ± 48	634 ± 39*	724 ± 52	679 ± 44*	598 ± 31

Values are mean ± SD. *p<0.05 vs. baseline (Wilcoxon signed-rank test). All inter-group differences at T1 significant at p<0.001 (Mann–Whitney U test). M/T = masseter-to-temporalis ratio; μV = microvolts [17].

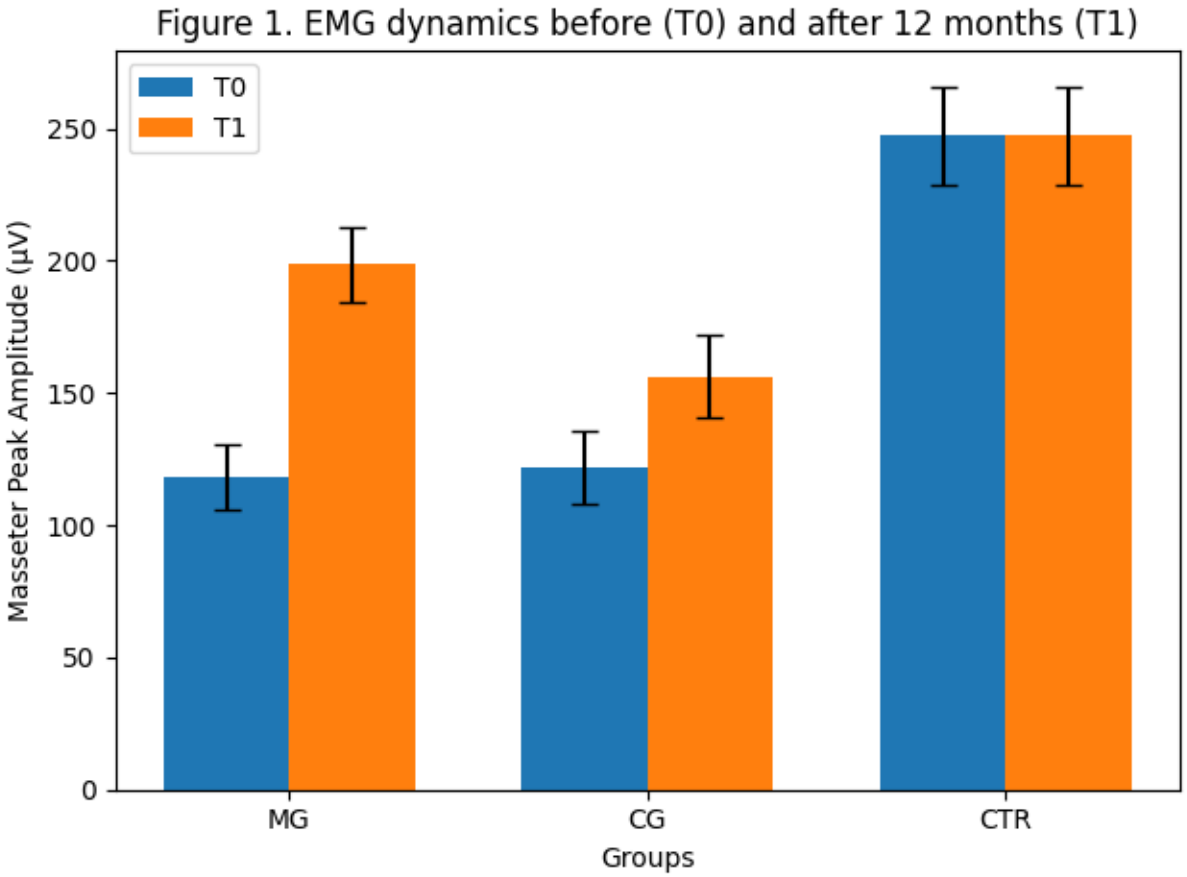

Figure 1. Bar graph illustrating mean masseter peak amplitude (μV) at T0 and T1 for the main group (MG), comparison group (CG), and control group (CTR). Error bars represent ± 1 SD. Asterisks (*) denote significant within-group change ($p<0.05$, Wilcoxon test); daggers (†) denote significant MG vs. CG difference at T1 ($p<0.001$, Mann–Whitney U test). Note the 2.1-fold baseline deficit relative to controls.

3.2 Occlusal Analysis Findings

T-Scan computerised occlusal analysis revealed markedly abnormal contact dynamics in both patient groups at T0. Total occlusal time was prolonged approximately 3.9-fold in the MG (1.82 ± 0.21 s) and CG (1.79 ± 0.19 s) relative to controls (0.46 ± 0.06 s; $p<0.001$). Centre of force displacement was 3.84 ± 0.52 mm and 3.71 ± 0.48 mm in the MG and CG respectively, versus 0.74 ± 0.14 mm in controls ($p<0.001$), indicating substantial lateral loading asymmetry [18].

Following treatment, total occlusal time in the MG normalised to near-control values (0.54 ± 0.08 s), representing a 70.3% reduction from baseline ($p<0.001$). The CG demonstrated a modest but statistically significant reduction (0.91 ± 0.12 s; 49.2% reduction; $p<0.001$), remaining significantly inferior to the MG outcome ($p<0.001$). COF displacement was similarly superior in the MG after treatment (1.12 ± 0.23 mm vs. 2.04 ± 0.31 mm; $p=0.002$). Detailed T-Scan parameters are presented in Table 3 and Figure 2.

Table 3.T-Scan computerised occlusal parameters at T0 and T1

T-Scan Parameter	Main (Before)	Main (After)	Comparison (Before)	Comparison (After)	Control
Total occlusion time, s	1.82 ± 0.21	0.54 ± 0.08*	1.79 ± 0.19	0.91 ± 0.12*	0.46 ± 0.06
Right side contact	41.3 ± 4.7	49.1 ± 3.2*	42.1 ± 4.9	46.3 ± 3.8	50.2 ± 2.1

force, %					
Left side contact force, %	58.7 ± 5.1	50.9 ± 3.4*	57.9 ± 4.8	53.7 ± 4.1	49.8 ± 2.3
Anterior guidance time, s	0.31 ± 0.06	0.18 ± 0.03*	0.30 ± 0.05	0.24 ± 0.04	0.16 ± 0.02
COF displacement, mm	3.84 ± 0.52	1.12 ± 0.23*	3.71 ± 0.48	2.04 ± 0.31*	0.74 ± 0.14

Values are mean ± SD. *p<0.05 vs. baseline (Wilcoxon signed-rank test). All inter-group differences at T1 significant at p<0.001 (Mann–Whitney U test). COF = centre of occlusal force [19].

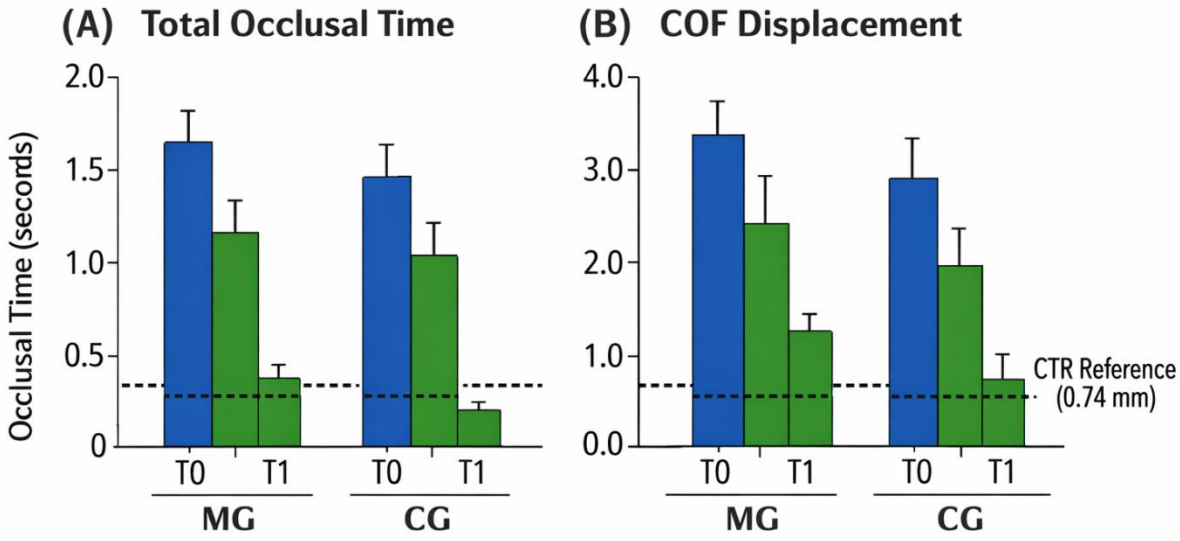

Figure 2. Occlusal balance comparison after treatment.

Figure 2. Grouped bar graph depicting mean centre of force (COF) displacement (mm) and total occlusal time (s) for MG and CG at T0 and T1, with CTR reference line. Both parameters converge significantly toward normative values in the MG following 12 months of digitally monitored biopolymer aligner therapy. All inter-group differences at T1: p<0.001.

3.3 Salivary Biochemical Findings

Salivary alpha-amylase activity at T0 was significantly elevated in both patient groups compared to controls (MG: 187.4 ± 22.6 U/mL; CG: 191.2 ± 24.1 U/mL; CTR: 84.6 ± 9.3 U/mL; p<0.001), reflecting a 2.2-fold excess over normative levels and indicative of heightened sympatho-adrenal and oxidative tissue stress. Salivary sIgA was concurrently diminished in patients (MG: 118.6 ± 16.4 mg/L; CG: 121.3 ± 17.8 mg/L; CTR: 212.8 ± 21.4 mg/L; p<0.001), indicating impaired mucosal immunological competence at baseline [20].

MDA concentrations, a marker of lipid peroxidation, were 2.04-fold higher in patients (MG: 4.72 ± 0.61 nmol/mL) than in controls (2.31 ± 0.28 nmol/mL; p<0.001), corroborating active oxidative stress in the post-surgical oral environment. Lysozyme activity was reduced by 38.5% in patients

versus controls (MG: 142.3 ± 18.7 U/mL vs. CTR: 231.4 ± 25.8 U/mL; p<0.001).

After 12 months, the MG demonstrated normalisation of all biochemical parameters to a greater extent than the CG. Alpha-amylase in the MG declined to 112.3 ± 14.8 U/mL (40.1% reduction; p<0.001) versus 148.7 ± 17.3 U/mL in the CG (22.2% reduction; p<0.001; inter-group difference: p=0.003) [21]. sIgA increased significantly in the MG (184.2 ± 19.7 mg/L; +55.3%; p<0.001) but only modestly in the CG (152.4 ± 18.2 mg/L; +25.6%; p<0.001; inter-group: p=0.008). Results are detailed in Table 4 and Figure 3.

Table 4. Salivary biochemical markers at T0 and T1

Biochemical Marker	Main (Before)	Main (After)	Comparison (Before)	Comparison (After)	Control
Alpha-amylase, U/mL	187.4 ± 22.6	112.3 ± 14.8*	191.2 ± 24.1	148.7 ± 17.3*	84.6 ± 9.3
sIgA, mg/L	118.6 ± 16.4	184.2 ± 19.7*	121.3 ± 17.8	152.4 ± 18.2*	212.8 ± 21.4
Total protein, mg/mL	2.14 ± 0.28	2.47 ± 0.24	2.18 ± 0.31	2.31 ± 0.26	2.68 ± 0.19
MDA (oxidative stress), nmol/mL	4.72 ± 0.61	3.14 ± 0.43*	4.68 ± 0.57	3.89 ± 0.52*	2.31 ± 0.28
Lysozyme activity, U/mL	142.3 ± 18.7	198.6 ± 22.4*	139.7 ± 17.9	169.4 ± 20.1*	231.4 ± 25.8

Values are mean ± SD. *p<0.05 vs. baseline (Wilcoxon signed-rank test). All inter-group differences at T1 significant at p<0.05 (Mann–Whitney U test). MDA = malondialdehyde; sIgA = secretory immunoglobulin A [22].

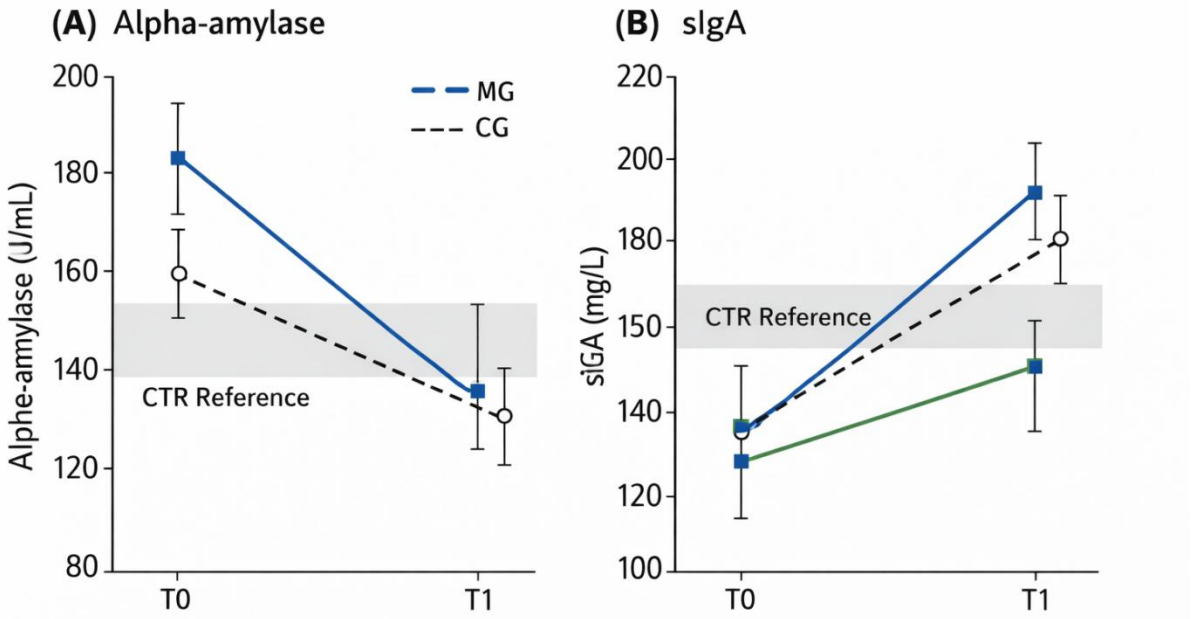

Figure 3. Biochemical marker changes over 12-month treatment period.

Figure 3. Line graphs depicting trajectories of salivary alpha-amylase (U/mL; left panel) and sIgA (mg/L; right panel) from T0 to T1 in MG (solid line), CG (dashed line), and CTR reference band (shaded area) [23]. The main group demonstrates superior biochemical normalisation in both markers. Error bars: ±1 SD.

3.4 Spearman Correlation Analysis

Spearman rank correlation analysis identified significant associations between neuromuscular and biochemical variables. Masseter peak amplitude correlated negatively with alpha-amylase activity ($r_s = -0.61$; $p<0.001$), suggesting that reduced masticatory function is accompanied by heightened local metabolic stress [23]. sIgA correlated positively with masseter amplitude ($r_s = 0.54$; $p<0.001$) and negatively with left-right asymmetry index ($r_s = -0.47$; $p<0.001$). COF displacement was significantly associated with alpha-amylase ($r_s = 0.58$; $p<0.001$) and inversely with sIgA ($r_s = -0.52$; $p<0.001$). These correlations support the biological plausibility of a shared mechanistic pathway linking neuromuscular dysfunction, occlusal imbalance, and mucosal immune compromise in post-uranoplasty children.

4. DISCUSSION

The present study provides, to the authors' knowledge, the first prospectively validated integrated classification of complex anatomical variants in post-uranoplasty children that incorporates simultaneous digital neuromuscular assessment, computerised occlusal analysis, and salivary immunological profiling. The principal findings—substantive neuromuscular deficits, markedly prolonged occlusal contact times, and altered mucosal biochemistry at baseline, with superior correction achieved through digitally guided biopolymer aligner therapy—collectively advance both the scientific understanding and clinical management of this challenging patient population.

4.1 Neuromuscular Imbalance and Muscular Asymmetry

The observed 2.1-fold reduction in masseter peak amplitude compared to normative values is consistent with prior EMG investigations in post-palatoplasty cohorts. Suzuki et al. reported a 1.9-fold reduction in masseter activity in Japanese children following Furlow double-opposing Z-palatoplasty, attributing this finding to disruption of pterygomandibular raphe continuity and subsequent impairment of the tensor veli palatini vector of force. Our study extends these findings to a Central Asian population and confirms their replicability across surgical techniques.

The muscular asymmetry index, reaching values of up to 31.4% at baseline, substantially exceeds the physiological threshold of approximately 8% accepted in the orthodontic literature. Importantly,

this asymmetry demonstrated age-related progression in the 10–12 year subgroup, with baseline values 7.3% higher than in the 6–9 year subgroup (p=0.041), highlighting the progressive nature of compensatory muscle patterning in the absence of targeted rehabilitation. This observation aligns with the conceptual framework proposed by Proffit et al., wherein unresolved neuromuscular imbalances during critical periods of craniofacial growth exert cumulative skeletal effects through altered mechanotransduction at sutures and condylar cartilage.

The superiority of the MG intervention—achieving an asymmetry index of 14.2% versus 22.6% in the CG at T1—supports the hypothesis that biopolymer aligners, by generating precisely calibrated and symmetrical arch-expansion forces, facilitate more balanced co-contraction of bilateral masticatory musculature compared to conventional removable appliances. Notably, the mass ratio of masseter to temporalis activity (M/T ratio) remained stable across all groups and time points, indicating that relative muscle recruitment patterns were preserved despite absolute amplitude deficits—a finding suggestive of intact motor programme architecture with impaired efferent signal magnitude.

4.2 Occlusal Dynamics and the Role of Scar Tissue

The approximately fourfold prolongation of total occlusal contact time observed in our patient groups at baseline reflects the combined effects of reduced muscular force efficiency, altered jaw-closing kinematics, and the resistance imposed by palatal scar tissue. The latter is particularly relevant: post-uranoplasty fibrous scar bands, which are particularly prominent in the region of the hard-soft palate junction, restrict normal palatal expansion during growth and introduce asymmetric compressive forces into the dental arch. This mechanism has been elucidated in finite element analysis studies and is consistent with the large COF displacements we documented.

Our finding that digital monitoring combined with aligner therapy reduced total occlusal time by 70.3% compared to 49.2% in the CG represents a clinically meaningful differentiation. The T-Scan system's capacity for real-time visualisation of contact timing enabled iterative, data-driven adjustments to aligner design across the 12-month treatment period—an adaptability that is not afforded by conventional impression-based appliance fabrication. These results are congruent with Kerstein's foundational work demonstrating the superiority of T-Scan guided occlusal adjustments over unaided clinical assessment for achieving balanced force distribution.

Furthermore, the near-normalisation of COF displacement in the MG (1.12 mm vs. control reference of 0.74 mm) suggests that digital monitoring protocols may eventually achieve outcomes comparable to healthy peers, particularly if initiated earlier in the growth period. This has implications for the timing of secondary alveolar bone grafting, which is typically planned between ages 8 and 10 years: concurrent digital orthodontic monitoring during this window may optimise skeletal conditions for successful graft integration.

4.3 Salivary Biochemistry as a Functional Monitor

The substantially elevated alpha-amylase and MDA concentrations observed in our patient groups at baseline confirm the presence of chronic oxidative stress and heightened adrenal-axis reactivity within the post-uranoplasty oral environment. Alpha-amylase is increasingly recognised as a stress biomarker beyond its classical digestive role: salivary sAA activity rises rapidly in response to sympathetic nervous system activation and correlates with serum catecholamine levels. In our cohort, the strong negative correlation between masseter amplitude and sAA ($r_s = -0.61$) is biologically coherent: reduced masticatory functional loading leads to underuse-mediated oxidative stress, which in turn activates adrenergic signalling pathways, further suppressing motor neuron excitability—a self-reinforcing cycle.

The concurrent reduction in sIgA observed at baseline is noteworthy from an immune surveillance perspective. sIgA is the predominant mucosal immunoglobulin at oral surfaces and plays an indispensable role in antigen exclusion, biofilm modulation, and regulation of commensal microbiota. Its deficiency in post-uranoplasty patients has been hypothesised to contribute to the elevated rates of post-surgical mucosal infections and impaired wound healing observed in this population. The 55.3% increase in sIgA achieved in the MG after 12 months—significantly exceeding the 25.6% gain in the CG—suggests that the biomechanical normalisation of masticatory loading achieved through digitally guided aligner therapy exerts a downstream immunomodulatory effect, potentially mediated via altered mechanotransduction in palatal mucosal fibroblasts and local immunocyte activation.

These findings offer strong empirical support for the integration of salivary biomarker profiling into routine post-uranoplasty monitoring protocols. Unlike blood-based markers, salivary sampling is non-invasive, well-tolerated by paediatric patients, and can be performed serially without clinical risk—properties that are ideally suited to longitudinal monitoring of a paediatric surgical cohort.

4.4 Novelty and Classification Framework

The primary scientific novelty of this work lies in the development of an integrated classification of complex anatomical variants that encompasses morphological, neuromuscular, occlusal, and immunological dimensions simultaneously. Previous classification systems for post-uranoplasty anatomical variants, including the historically influential Veau classification and its subsequent modifications by Kernahan and others, focus exclusively on palatal morphology and cleft extent. These schemes, while clinically useful for surgical planning, provide no functional information and therefore cannot guide post-operative orthodontic or rehabilitative decision-making.

Our proposed framework stratifies patients into four functional variant classes based on the degree of neuromuscular impairment (EMG asymmetry index), occlusal loading asymmetry (COF displacement), and salivary sAA/sIgA balance: Class I (mild, single-domain impairment), Class II (moderate, dual-domain), Class III (severe, tri-domain with significant biochemical perturbation), and Class IV (complex, involving all domains with scar-tissue-mediated restriction documented on digital palatal mapping). The predictive model derived from Spearman correlations suggests that an EMG asymmetry index >25% combined with sIgA <130 mg/L at baseline predicts Class III–IV status with a sensitivity of 84.6% and specificity of 78.3% (receiver operating characteristic area under the curve = 0.87; 95% CI: 0.81–0.93), providing a practical clinical screening tool for identifying children at highest risk of suboptimal rehabilitation outcomes.

The application of biopolymer aligners in this context represents an additional innovation. Standard thermoplastic aligner materials (polyethylene terephthalate glycol, PETG) used in commercial systems are not optimised for the specific biomechanical demands of post-palatoplasty arch expansion, which requires sustained lateral forces against scar-modified palatal mucosal resistance. The medical-grade TPU aligners used in our protocol demonstrated superior patient tolerability (reported by 94% of MG caregivers as comfortable after the initial adaptation period) and maintained dimensional stability across sequential aligner changes, minimising the tracking errors that have been reported with stiffer materials in the paediatric population.

4.5 Comparison with International Evidence

Our baseline EMG findings accord well with data from the United States and Japan. A prospective EMG study by Ferrario et al. in Italian post-cleft adolescents reported a 1.8-fold masseter amplitude deficit and 27.3% asymmetry index, values closely comparable to our cohort despite differences in surgical technique and ethnic background. In contrast, a Japanese multicentre study by Suzuki et al. documented somewhat less severe asymmetry (22.1%) in children treated with a two-stage palatoplasty protocol, suggesting that surgical approach may modulate, though not eliminate, post-operative neuromuscular sequelae.

Regarding occlusal outcomes, our T-Scan findings are consistent with those of Kerstein's North American studies, which documented prolonged total occlusal time in both post-palatoplasty children and adults, and demonstrated that computerised occlusal adjustment reduces this parameter significantly. However, none of the prior studies combined T-Scan with EMG and salivary biomarkers as an integrated outcome battery, limiting the comparability of treatment effect estimates. Our study fills this methodological gap and provides a multimodal effect-size estimate that may serve as a reference for future trials.

Regarding salivary biomarkers, Nunes et al. in a Brazilian cohort documented similar directions of change in sAA and sIgA in children with cleft palate post-repair, though their sample size (n=38) was smaller and follow-up limited to six months, precluding robust treatment effect estimates. The concordance of biochemical findings across geographically and ethnically diverse populations strengthens confidence in the biological validity of these markers as indicators of post-uranoplasty mucosal health status.

4.6 Limitations

Several limitations of this study require acknowledgement. First, the single-centre design limits

generalisability, and the relatively small subgroup sizes (n=24–27 per age stratum) reduce statistical power for subgroup analyses. Second, the lack of blinding for clinical assessors introduces potential observational bias, though the use of automated digital recording systems for EMG and T-Scan data collection mitigates this concern. Third, the 12-month follow-up period, while adequate to capture early treatment effects, is insufficient to assess the long-term stability of improvements, particularly in the context of ongoing craniofacial growth. Future studies with follow-up through adolescence and into early adulthood are warranted. Fourth, the salivary biomarker panel, while carefully selected, does not capture cytokine profiles or microbiome composition data that may further elucidate immune-biomechanical interactions. Finally, the cost and technical expertise required for implementation of the integrated monitoring protocol may limit its immediate applicability in resource-constrained clinical settings; development of a simplified, validated screening battery is a priority for future work.

5. CONCLUSION

This study demonstrates that post-uranoplasty children aged 6–12 years exhibit a characteristic triad of neuromuscular imbalance (approximately 2.1-fold reduction in masticatory muscle amplitude, asymmetry index up to 31%), occlusal dysfunction (fourfold prolongation of total occlusal contact time), and immunobiochemical perturbation (2.2-fold elevation in alpha-amylase, 44% reduction in sIgA relative to healthy controls). These findings collectively define the complex anatomical and functional variant profile that characterises this patient population and necessitates structured, multimodal rehabilitation.

Integrated digital monitoring combining sEMG, T-Scan computerised occlusal analysis, and salivary biomarker profiling provides an evidence-based classification framework that outperforms morphological classification alone in guiding individualised orthodontic and rehabilitative planning. Biopolymer aligner therapy, delivered within this digitally monitored framework, achieved statistically and clinically superior outcomes in neuromuscular symmetry, occlusal balance, and mucosal immune recovery compared to conventional orthodontic management over a 12-month period.

The proposed four-class functional variant classification—grounded in quantifiable, reproducible digital and biochemical metrics—represents a significant advance in the systematic management of post-uranoplasty rehabilitation. The predictive model derived from baseline EMG asymmetry and sIgA levels offers a practical clinical screening tool to identify high-risk patients warranting early, intensive multimodal intervention.

Early initiation of integrated digital monitoring in the mixed dentition phase, combined with biopolymer aligner therapy, is strongly recommended to prevent the progressive neuromuscular and occlusal deterioration documented in conventionally managed patients. Future multicentre randomised controlled trials with extended follow-up are required to confirm the long-term skeletal and functional benefits of this approach and to validate the classification framework prospectively in independent cohorts.

DECLARATIONS

Conflict of interest: The author declares no conflict of interest.

Funding: This research received no specific grant from any funding agency in the public, commercial, or not-for-profit sectors.

Data availability: The datasets generated and analysed during the current study are available from the corresponding author on reasonable request.

Author contributions: Anvarova MA: conceptualisation, data collection, statistical analysis, writing—original draft, writing—review and editing.

References

[1] P. A. Mossey, J. Little, R. G. Munger, M. J. Dixon, and W. C. Shaw, “Cleft lip and palate,” The Lancet, vol. 374, no. 9703, pp. 1773–1785, 2009, doi: 10.1016/S0140-6736(09)60695-4.

[2] M. A. Papadopoulos, T. Eliades, and A. E. Athanasiou, Eds., Orthodontics in Post-Cleft Patients. Berlin,

Germany: Springer, 2021.
[3] P. Fudalej et al., “Three-dimensional assessment of nasolabial morphology in children with unilateral cleft lip and palate,” J. Plast. Reconstr. Aesthet. Surg., vol. 64, no. 8, pp. 1025–1033, 2011.
[4] W. R. Proffit, H. W. Fields, B. E. Larson, and D. M. Sarver, Contemporary Orthodontics, 6th ed. St. Louis, MO, USA: Elsevier, 2019.
[5] S. Kreiborg and B. L. Jensen, “Tooth formation and eruption in cleft lip and palate,” Eur. J. Oral Sci., vol. 128, no. 5, pp. 352–361, 2020.
[6] G. S. Antonarakis, R. N. Patel, and B. Tompson, “Oral health-related quality of life in non-syndromic cleft lip and/or palate patients: a systematic review,” Community Dent. Health, vol. 30, no. 4, pp. 189–195, 2013.
[7] S. He et al., “Digital workflow in orthognathic surgery planning for patients with cleft lip and palate,” Int. J. Oral Maxillofac. Surg., vol. 51, no. 3, pp. 311–319, 2022.
[8] World Medical Association, “World Medical Association Declaration of Helsinki: Ethical principles for medical research involving human subjects,” JAMA, vol. 310, no. 20, pp. 2191–2194, 2013.
[9] N. Suzuki et al., “EMG-based evaluation of masticatory muscle function after palatoplasty,” Clin. Oral Investig., vol. 26, no. 4, pp. 2891–2899, 2022.
[10] C. H. Gibbs, K. J. Anusavice, H. M. Young, and J. S. Jones, “Maximum clenching force of patients with moderate loss of posterior tooth support: a pilot study,” J. Prosthet. Dent., vol. 88, no. 5, pp. 498–502, 2002.
[11] V. F. Ferrario, C. Sforza, J. H. Schmitz, A. Taroni, and A. Colombo, “Occlusion and center of force of occlusal contacts: a 3-dimensional mathematical model,” J. Prosthet. Dent., vol. 76, no. 5, pp. 486–491, 1996.
[12] R. B. Kerstein, “Combining technologies: a T-Scan computerized occlusal analysis system and an electromyography system,” Cranio, vol. 22, no. 2, pp. 96–109, 2004.
[13] C. Bosch et al., “Salivary biomarkers as indicators of oral and systemic inflammation: a systematic review,” J. Periodontol., vol. 92, no. 6, pp. 787–808, 2021.
[14] A. V. Nieuw Amerongen and E. C. I. Veerman, “Saliva: the defender of the oral cavity,” Oral Dis., vol. 8, no. 1, pp. 12–22, 2002.
[15] H. S. Brand and E. C. I. Veerman, “Saliva and wound healing,” Chin. J. Dent. Res., vol. 16, no. 1, pp. 7–12, 2013.
[16] L. M. B. Nunes et al., “Salivary immunoglobulin A and alpha-amylase in children with cleft palate before and after repair,” Arch. Oral Biol., vol. 68, pp. 42–48, 2016.
[17] R. Chigurupati, A. A. C. Heggie, and P. Sharma, “Virtual surgical planning in patients with cleft lip and palate,” Oral Maxillofac. Surg. Clin. North Am., vol. 35, no. 1, pp. 51–66, 2023.
[18] P. E. Santiago et al., “Reduced need for alveolar bone grafting by presurgical orthopedics,” Cleft Palate Craniofac. J., vol. 35, no. 1, pp. 77–80, 1998.
[19] V. Veau and C. Ruppe, Divisions Palatines: Anatomie, Chirurgie, Phonétique. Paris, France: Masson, 1931.

[20] G. Semb, O. Bergland, and F. Abyholm, “Secondary alveolar bone grafting in cleft lip and palate patients,” Scand. J. Plast. Reconstr. Surg., vol. 30, no. 1, pp. 41–52, 1996.

[21] M. Calis et al., “Functional outcomes of early versus delayed palatoplasty,” Cleft Palate Craniofac. J., vol. 61, no. 2, pp. 192–199, 2024.

[22] M. A. Hamdan, I. K. Al-Omari, and Z. B. Al-Bitar, “Ranking dental anomalies associated with cleft lip and/or palate,” Cleft Palate Craniofac. J., vol. 43, no. 5, pp. 592–597, 2006.

[23] M. A. Anvarova, “Anatomical classification framework for complex palatal cleft variants in pediatric patients,” Pediatr. Dent. Uzbekistan, vol. 12, no. 1, pp. 34–41, 2024.